AGU ADVANCING EARTH AND SPACE SCIENCES

Geophysical Research Letters

RESEARCH LETTER
10.1029/2024GL109675

Overestimation of Mangroves Deterioration From Sea Level Rise in Tropical Deltas

Zhijun Dai[1,2], Chuqi Long[1], Xuefei Mei[1], Sergio Fagherazzi[3], and Yuan Xiong[1]

[1]State Key Laboratory of Estuarine and Coastal Research, East China Normal University, Shanghai, China, [2]Laboratory for Marine Geology, Qingdao Marine Science and Technology Center, Qingdao, China, [3]Department of Earth and Environment, Boston University, Boston, MA, USA

Key Points:

- Mangroves along typical deltas are expanding seaward of about 18% ± 12% m/yr, indicating that there is little impacts from sea level rise
- Mangrove expansion here can efficiently offset 67% landward mangrove losses
- New model project that 90% of mangrove fringes may start retreating within 132–194 years, and wave-dominated delta present early inundation

Supporting Information:

Supporting Information may be found in the online version of this article.

Correspondence to:

Z. J. Dai,
zjdai@sklec.ecnu.edu.cn

Citation:

Dai, Z., Long, C., Mei, X., Fagherazzi, S., & Xiong, Y. (2024). Overestimation of mangroves deterioration from sea level rise in tropical deltas. *Geophysical Research Letters*, *51*, e2024GL109675. https://doi.org/10.1029/2024GL109675

Received 11 APR 2024
Accepted 26 SEP 2024

Author Contributions:

Conceptualization: Zhijun Dai
Data curation: Zhijun Dai, Chuqi Long, Xuefei Mei
Formal analysis: Zhijun Dai, Chuqi Long, Sergio Fagherazzi
Funding acquisition: Zhijun Dai, Sergio Fagherazzi
Investigation: Zhijun Dai, Chuqi Long, Xuefei Mei, Sergio Fagherazzi, Yuan Xiong
Methodology: Zhijun Dai
Project administration: Zhijun Dai
Resources: Zhijun Dai, Chuqi Long, Xuefei Mei, Yuan Xiong
Software: Zhijun Dai, Sergio Fagherazzi
Validation: Zhijun Dai
Visualization: Zhijun Dai
Writing – original draft: Zhijun Dai

Abstract Mangrove forests are critical coastal ecosystems that provide great socio-ecological services, which are also highly vulnerable to climate change, particularly to sea level rise (SLR). Here we assess changes in mangrove forests in four distinct river/tide/wave-dominant large deltas along the Indo-Pacific coast based on 1,336 remote sensing images by machine learning techniques. We find that mangroves are migrating seaward at a rate of 18% ± 12% m/yr, which can offset landward mangroves loss, 67% of which caused by land use conversion. The fact that mangroves are expanding seaward with accretion rates exceeding SLR suggests that climate change has not yet triggered substantial loss in deltaic mangrove forests. Assuming that present environmental conditions do not change and that sediment and organic deposition in the deltaic topsets match SLR rates, we project that 90% of deltaic mangrove forests may start to retreat after 132–194 years. Early inundation of mangroves will occur in wave-dominated delta.

Plain Language Summary Mangrove forests provide significant ecological and societal services, and mitigation global warming. However, large-scale loss in mangroves could be induced by anthropogenic drivers and sea level rise (SLR). Our study based on deltas along the Indo-Pacific coast, highlight that mangroves are expanding seaward at a rate of 18% ± 12% m/yr, indicating that there is little impacts from SLR and has not been substantial loss in mangrove forests in these deltas so far. Mangrove expansion here can efficiently offset 67% landward mangrove losses indicates that our new model project that 90% of mangrove shorelines will may start retreating within 132–194 years. We conclude that favoring mangroves expansion seaward would enhance coastal protection and reduce the need of landward mangrove restoration.

1. Introduction

Mangrove forests, present along tropical and subtropical shorelines, provide significant ecological and societal services (Duke et al., 2007; Woodroffe et al., 2016), including coastal protection (Zhou et al., 2022), blue carbon sequestration (Duarte et al., 2013), and fisheries support (Aburto-Oropeza et al., 2008). Despite the importance of their ecological services, mangrove forests have declined by 30%–50% over the past half century (FAO, 2007), and deforestation continues at an annual rate ranging between 0.16% and 0.39% since 2000 (Hamilton & Casey, 2016). Urbanization of the shoreline and land-use change driven by agriculture and aquaculture directly induce large-scale degradation of the global mangroves stock (Friess et al., 2019). Insufficient fluvial sediment supply caused by damming might slow accretion in mangrove forests, possibly triggering ecosystem degradation, while seawalls and dykes parallel to the shoreline will hamper the landward expansion of mangroves (Murray et al., 2019, 2022; Schuerch et al., 2018; Tamura et al., 2020).

Furtherly, while the vertical accretion ability of mangroves cannot match sea level rise (SLR), possible wide-spread mangrove loss will be found in the near future (Blankespoor et al., 2014; Lovelock et al., 2015; Spencer et al., 2016). Recent work in the Indo-Pacific shows that in 69% of 27 mangrove sites SLR exceeds the soil surface elevation gain (Lovelock et al., 2015), indicating that mangrove could face the drowning risk from SLR. However, it can note that the persistence of mangroves along coastlines implies their ability to cope with moderate rates of SLR (Woodroffe et al., 2016). Furtherly, mangrove forests can continue to colonize seaward when sediment supply is sufficient or there is broad bare tidal flat in front of the mangroves (Asbridge et al., 2016; Godoy & Lacerda, 2015; Long et al., 2022; Lovelock et al., 2010; Willemsen et al., 2016). Therefore, although large-scale mangrove loss was be driven by anthropogenic stress, limited information reveals whether mangrove wetland can keep pace with SLR or not.

Writing – review & editing: Zhijun Dai, Sergio Fagherazzi

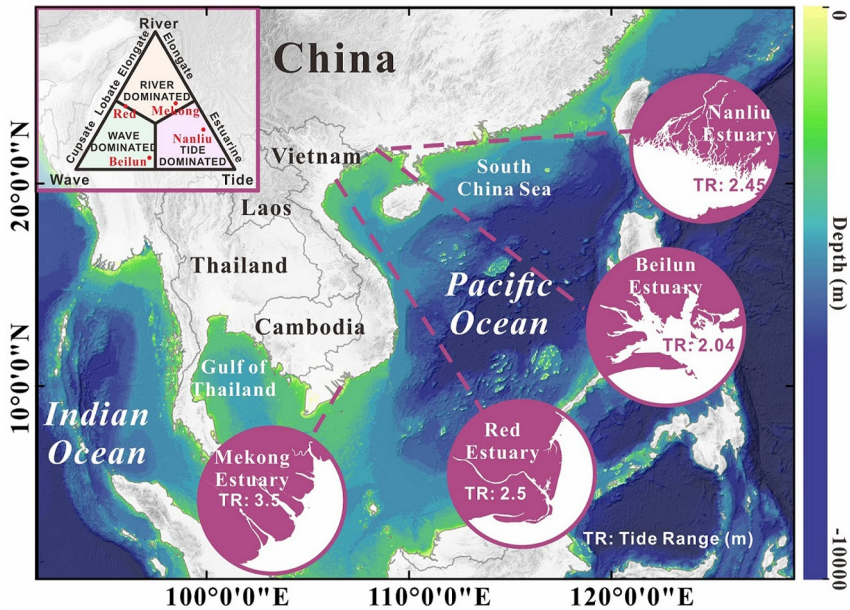

Figure 1. Map of study area along the Indo-Pacific. Location of four mangrove dominated deltas, including Manliu delta, Beilun delta, Red delta, and Mekong delta.

Here we present new evidence on demonstration that mangrove forest extent and associated seaward/landward migration between 1986 and 2020 in deltas along the Northwest Pacific coast could experience distinct changes despite SLR. Deltaic regions host most of the world's mangrove forest by accounting for about 40.5% (54,972 km^2) of the total mangrove area (Giri et al., 2011; Lovelock et al., 2015; Worthington et al., 2020). The Nanliu, Beilun, Red, and Mekong deltas where selected to account for variations in rates of sea-level rise, tidal range, wave regime, fluvial discharge, and anthropogenic disturbance. These 4 deltas represent tide-dominated, wave-dominated, rive and wave dominated and river-dominated, respectively (Figure 1). Using 1,336 Landsat scenes combined to records of sediment discharge delivered to the delta, we map (a) loss and gain in mangrove area to discern which driver is dominant and (b) retreat or advance in mangrove shoreline to determine whether the mangroves can survive SLR. Assuming that the present conditions will be maintained, we present a new model to project deposition rates of deltaic mangroves and compare them to SLR. Our results broaden our understanding of mangrove forest dynamics and provide key data sets for mangrove-based protection against future flooding.

2. Methods

2.1. Extraction of Temporal and Spatial Distribution of Mangrove Forest and Bare Tidal Flat

A total of 1,336 Landsat remote sensing imageries between 1986 and 2020 were utilized to extract the spatial distribution of mangrove forest in 4 deltas, which can be freely accessed and queried through Google Earth Engine (https://code.earthengine.google.com/) (Figure S1 in Supporting Information S1). Four effective spectral indexes were served as auxiliary inputs into the Random Forest classifier to enhance the classification (Table S2 in Supporting Information S1). Since the visible extent of bare tidal flats depends on the tide levels, a total of 20 cloud-free images taken at around the same tide level were selected for analysis of the seaward margin of bare tidal flat. Yearly sediment discharge and tidal level data were collected from BeiHai, HonDua, and VungTau stations (Tables S3 and S4 in Supporting Information S1), provided by the Permanent Service for Mean Sea Level (PSMSL) (https://psmsl.org/data/) and Mekong River Commission (MRC) (https://portal.mrcmekong.org/, upon registration/login). To quantify changes in mangroves and bare tidal flats, we calculated the historical shoreline change rate with DSAS (https://www.usgs.gov/centers/whcmsc/science/digital-shoreline-analysis-system-dsas), representing the average annual seaward transgression of mangroves and adjacent flats (Himmelstoss et al., 2021) (Figure S1 in Supporting Information S1).

2.2. Calculation of the Mangrove Forests Submergence in Different SLR Scenarios

ETOPO 2022 is an earth surface elevation data set (NOAA National Centers for Environmental Information) (https://www.ncei.noaa.gov/products/etopo-global-relief-model), generated from NASA's ICESat-2 satellite elevation images with a resolution of 15 arc-second. The vertical mean bias error is 0.12 ± 0.75 m and the overall root mean square error is 0.76 m (Amante et al., 2023). This data set was only used to calculate the slope $\tan\theta$ of each DSAS transect (Figures S2 and S3 in Supporting Information S1). The average slope of the 4 deltas (Nanliu, Beilun, Red, and Mekong) is 0.00413°, 0.042°, 0.00297°, and 0.00257°, respectively.

According to the Intergovermental Panel on Climate Change (IPCC) 6th Assessment Report (AR6), future sea level change can be cataloged in six scenarios based on projected Greenhouse Gas Emissions: very low rate of SLR (SSP1-1.9), low (SSP1-2.6), intermediate (SSP2-4.5), high (SSP3-7.0), and very high (SSP5-8.5) (IPCC, 2022) (https://sealevel.nasa.gov/ipcc-ar6-sea-level-projection-tool). The annual mean SLR rates V_{slr} under the scenarios SSP1-2.6, SSP2-4.5, and SSP5-8.5 were selected in this study (Figure S4 and Table S3 in Supporting Information S1). The rate of annual sea level transgression (mean SLR projected along the horizontal direction) is V'_{slr}:

$$V'_{slr} = V_{slr}/\tan\theta$$

Considering both the bare flats and mangrove forest slopes θ.

Three possible scenarios are present for bare tidal flat variations in response to SLR: (a) with bare flat in front, if the vertical accretion rate of the bare flat is lower than SLR, the bare flat will become submerged; (b) without bare tidal flat, if the vertical accretion in the forest is lower than SLR, the mangroves will be submerged by the rising water levels; and (c) with a bare flat in front and both have an accretion rate below SLR (Figure S3 in Supporting Information S1), the bare flat is initially submerged, followed by the mangroves. Details of the calculation process are provided in Supporting Information S1: Auxiliary Methods.

Based on the above three scenarios, the time limit of mangrove forest expansion for each transects of the delta in response to the SLR scenarios of SSP1-2.6 (low), SSP2-4.5 (intermediate), and SSP5-8.5 (very high SLR) is calculated (IPCC, 2022). Then, the cumulative frequency of submergence time for all sections of each delta in the three scenarios is computed (Figure 4 and Figure S5 in Supporting Information S1). Finally, the relationship between cumulative frequency and submergence time is fitted using quadratic exponential function, with the fitting accuracy reaching the significance level of 0.01 (Tables S5 and S6 in Supporting Information S1). The time limit for the submergence of 75% and 90% of the entire deltaic mangroves area can be estimated through the fitting function.

3. Results

3.1. Dynamics in Mangrove Areas

Here, four deltaic mangrove forests are investigated, which represent riverine, wave and tidal end-members of world deltas (Dalrymple et al., 1992) (Figure 1a). We found that the total area of mangrove forests display a significant gain with average change rate of 80.8 ha/yr during 1986–2020 (Figure 2a), in contrast to previous work that reports a global loss of mangroves at a yearly rate of 34,700 ha between 1990 and 2020 (FAO, 2020). Further, the mangrove forest shorelines present an expansion rate of 18.9 m/yr over the past 35 years. Between 1986 and 2020, the area of mangrove forests in the tide-dominated Nanliu delta increased 25.31 ha/yr, while the mangroves of the Mekong, Red, and Beilun deltas have increased of 245.07, 45.03, and 7.66 ha/yr, respectively (Figure 2a and Table S7 in Supporting Information S1). Interannual variations in mangrove area are also present, indicating the occurrence of occasional loss along with long-term expansion. For instance, the mangrove forest in the Beilun delta covers 1,021 ha during 1990–1995, around 90% of the area measured in 1986, while mangroves in the Red and Mekong delta display a decrease of 21% and 4% in 2015 with respect to 2010 (Figure 2a and Table S7 in Supporting Information S1).

3.2. Spatial Distribution of Mangroves

The spatial distribution of mangrove forests in the 4 deltas is further analyzed every 5 years (Figure S6 in Supporting Information S1). Despite a net overall gain, the 4 deltas indicate large-scale local loss (Figures 2b and 3,

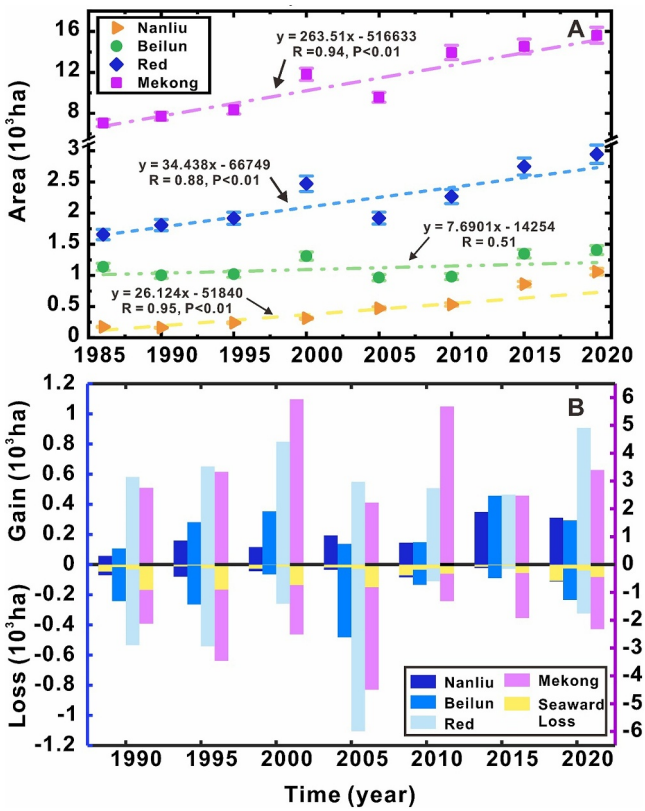

Figure 2. Changes of mangrove forest in four typical deltas (Nanliu, Beilun, Red, and Mekong) during the period of 1986–2020. (a) Changes in mangrove forest areas between 1986 and 2020. (b) Loss and gain of mangrove forest every 5 years in each delta.

Table S7 in Supporting Information S1). In 2005, mangrove forests in the Beilun, Red, and Mekong deltas even present net overall losses exceeding gains, with mangrove area much lower than in previous years (Figure 2b and Table S7 in Supporting Information S1). We note that mangroves loss is concentrated at the upland border, while gain mainly occurs at the ocean boundary, with local erosion sometimes occurring in areas open to the sea (Figure 3 and Figure S7 in Supporting Information S1). This trend is particularly obvious in the wave-dominated Red delta (Figure S7c in Supporting Information S1). When compared to 1986, both landward mangrove loss and seaward gain suggest seaward progradation of the deltas (Figure 3 and Figure S6–S8 in Supporting Information S1). The net variation of mangrove forest area is therefore a tradeoff between the seaward gain and landward loss.

3.3. Gain and Loss in Mangroves

We stress that mangrove forest losses are concentrated in the upland boundary, while the ocean margin mostly displays forest gains. On the basis of our analysis of 2,242 transects in 4 deltas at 100 m interval (Figure S2 in Supporting Information S1), we find that the loss of mangrove forest exceeds our expectations if we ignore the seaward mangrove expansion (Figure 3). The landward loss were 70, 455, 1,220, and 2,557 ha in Nanliu, Beilun, Red, and Mekong delta in the past 35 years, respectively (Table S8 in Supporting Information S1). We also found that the amount of gross loss or gain at a 5-year interval is much larger than the amount of overall net gain, thus displaying large oscillations, which means that overall mangrove loss of four delta is far below their areal variation (Tables S2–S4 in Supporting Information S1), and all 4 deltas exhibit mangrove gains (Table S7 in Supporting Information S1, Figure 2). In facts, while the area of mangrove forest in the Red delta presents a slight increase during 1986–1995 (Figure 2a), the loss of mangrove forest area in 1990 and 1995 is 534.35 and 541.42 ha when compared to 1986 and 1990, with a net gain of 47.94 and 110.08 ha (Figure 2b and Table S7 in Supporting Information S1). It is noted that 95% of the losses between 1986 and 2020 are concentrated at the upland boundary, likely due to deforestation.

Mangrove gains at the ocean margin and mangrove loss at the upland boundary are respectively 2,873.27 and 1,220.73 ha, with the gain accounting 85.90% of the total area in 2020 (Figure S9, Tables S8 and S9 in Supporting Information S1). Overall, mangroves are migrating seaward at a rate of 18% ± 12% m/yr (Table S10 in Supporting Information S1), which largely offsets the mangrove loss due to human intervention (Table S8 in Supporting Information S1). Nanliu delta has the highest migration rate with 33.41 m/yr, while the Mekong delta expands at a rate of only 15.55 m/yr. Approximately 80% of the mangroves' shorelines are expanding seaward, with a percentage of 92%, 81%, 80%, and 69% in Naliu, Beilun, Red, and Mekong delta, respectively, showing that deltas dominated by different dynamics are still expanding seaward in spite of SRL (Table S10 in Supporting Information S1).

In tide-dominated deltas, tidal currents transport abundant sediment to the estuary, enabling fringe mangrove forests to deposition and expand seaward with high deposition rate (Long et al., 2022). In river-dominate delta, the terrestrial sediment inputs are mainly delivered to the interior mangroves rather than the mangrove front. Barrier islands are the typical geomorphic feature of wave-dominated delta, which create a sheltered and low-energy environment for mangroves growth (Adame et al., 2010). The strong wave force induces sediment overwash through the barriers and deposit behind, proving significant materials for mangroves (Long et al., 2021). When the gaining elevation of mangrove forests through sediment trapping cannot keep pace with raising sea level, mangroves will be submerged and retreat (Lovelock et al., 2015; Saintilan et al., 2023).

Further, 54% of the original mangrove forests in 1986 has been eroded or converted to other land-use over the past 35 years in the 4 deltas, but the net area gain is 176% of the 1986 value (Figure 2b and Table S7 in Supporting Information S1), which is in contrast with a previous area loss estimation of 12% in Asia (FAO, 2020). The

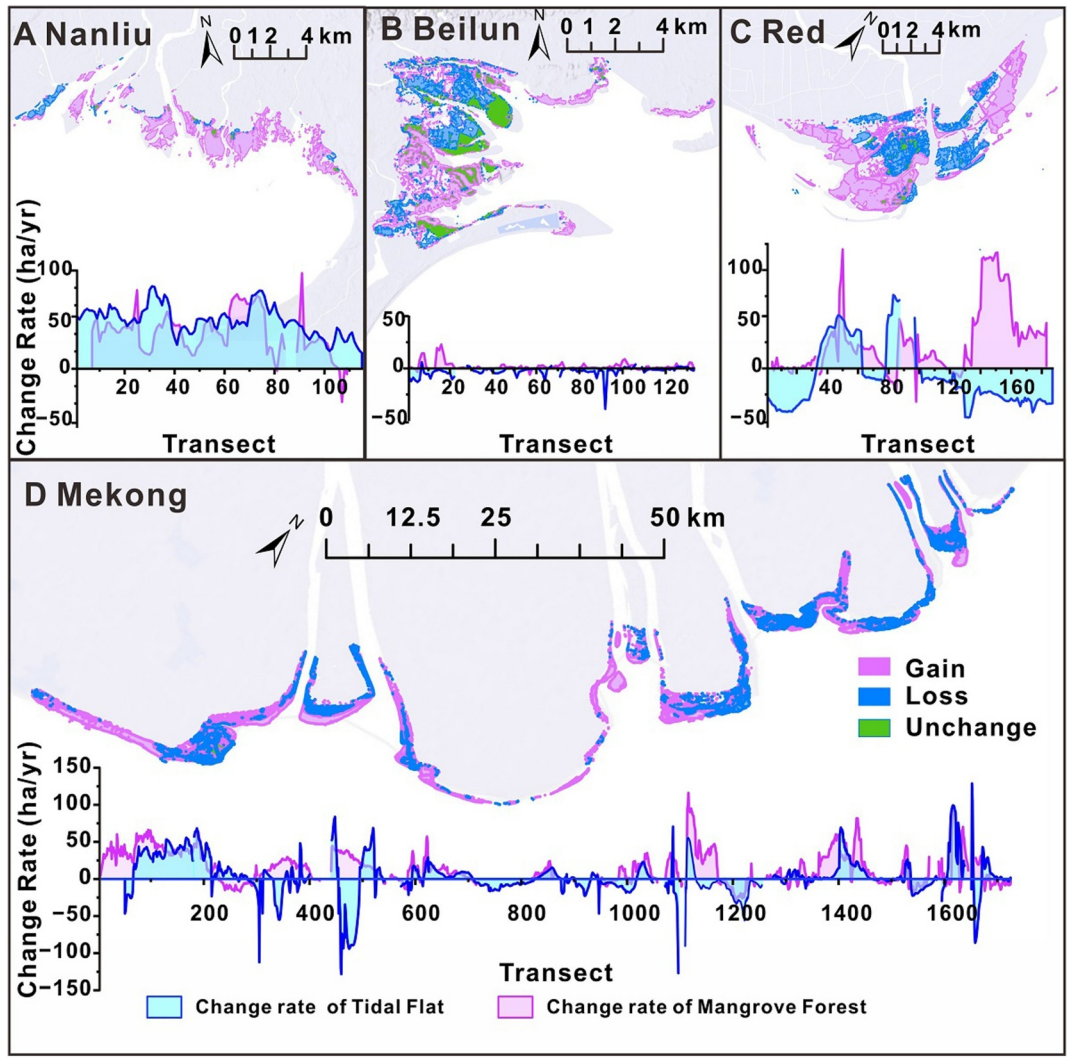

Figure 3. Delta images indicate the distribution of mangrove forest, with the green patches representing unchanged mangroves between 1986 and 2020, the purple and blue patches representing the gain and loss of mangroves, respectively. Curve graphs show the change rate of mangrove forest (color in purple) and bare tidal flats (color in blue). (a) Nanliu delta, (b) Beilun delta, (c) Red delta, and (d) Mekong delta.

anthropogenic inland losses were 70.88, 455.1, 1,220.73, and 2,557.81 ha in 4 deltas (Nanliu, Beilun, Red, and Mekong), which account for 67%, 97%, 94%, and 72% of the total loss in the period of 1986–2020 (Table S8 in Supporting Information S1). Although some losses of mangrove forest are present along the ocean boundary, the gained area seaward is about 12 times higher (Tables S8 and S9 in Supporting Information S1). Specifically, if we exclude the anthropogenic inland losses, the gained area of mangrove forests is larger than calculated. Therefore, the seaward expansion of mangroves compensates for the loss in the upland regions, and generates the illusion of an overall low rate of areal loss. Similarly, we find that the loss of mangrove forest is much higher without accounting for seaward progradation. When considering seaside gain and upland loss separately, we find that the seaside gain is 3 times the upland loss in the 4 deltas (Tables S7–S9 in Supporting Information S1).

4. Discussion

4.1. Impact of Suspended Sediment Discharge Reduction

Northwest Pacific mangroves are suffering from various anthropogenic disturbances, like deforestation, land reclamation, and shrimp farming (Adame et al., 2018; Gandhi & Jones, 2019). These activities are also

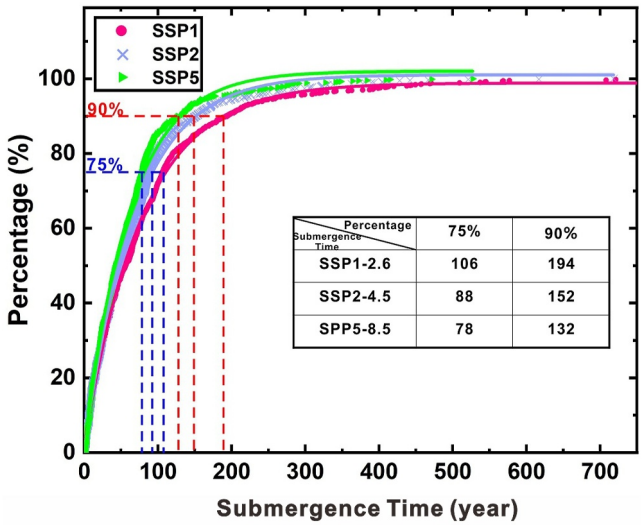

Submergence Time \ Percentage	75%	90%
SSP1-2.6	106	194
SSP2-4.5	88	152
SPP5-8.5	78	132

Figure 4. Submergence time of mangrove forest under three sea level rise scenarios published by IPCC: SSP1-2.6 (low), SSP2-4.5 (intermediate), and SSP5-8.5 (very high).

responsible for mangrove loss in the 4 deltas analyzed in this study (Figure 1). To save costs and maximize benefits, people typically cut the forest and reclaim land at the landward boundary; thus seaside mangroves are maintained because they are located far from human dwellings (Long et al., 2021).

In recent years it has been proposed that a sharp decline in sediment supply from rivers has triggered mangrove retreat (e.g., Hu et al., 2020; Long et al., 2021; Milliman & Farnsworth, 2011; Syvitski et al., 2009). In contrast to previous studies, here we indicate that: (a) mangrove loss mainly occurs at the landward boundary of deltas. We estimate an area loss of 4,300 ha at the landward boundary of the 4 deltas during 1986–2020 caused by anthropogenic land use conversion rather than a decline in riverine sediment (Figures S7, S9, and Table S8 in Supporting Information S1); (b) Seaward mangroves are more directly affected by riverine sediment supply and SLR. Over the past 35 years, the 4 deltas have gained 13,600 ha at the ocean margin, indicating that the decrease in suspended sediment discharge and the increase in sea level have not yet influenced these forests (Figure 3, Figures S10 and S11 in Supporting Information S1). We therefore stress that the attribution of mangrove loss to a decline in riverine suspended sediment discharge might be biased, since it ignores the spatial variation of mangrove areas, reclamation of mangrove forests at the land side, and gain-loss tradeoff.

4.2. Impact of Sea-Level Rise

Although deltaic mangroves are threatened by rapid sea-level rise, an increase in water level might induce landward migration of mangrove forests and possibly areal expansion (Friess et al., 2022; McIvor et al., 2013; McKee et al., 2007; Morris et al., 2002; Woodroffe et al., 2016). However, the landward expansion is likely constrained by topographic slope and human infrastructure (Schuerch et al., 2018). The rate of sea-level rise over the four deltaic regions have ranged between 77 and 109 mm over 1986–2020 while their tidal amplitudes are between 2.04 and 3.8 m (Figure S12 in Supporting Information S1). All the 4 deltas display seaward expansion of mangrove forest, rather than landward migration. In detail, mangroves in the Nanliu delta expanded of 25.3 ha/yr while in the Mekong, Beilun, and Red deltas prograded of 245.1, 7.7, and 45 ha/yr (Figures 2 and 3, Table S7 in Supporting Information S1). When considering the slope of nearby bare tidal flats, the rate of seaward migration suggests a vertical accretion rate that exceeds the rate of sea-level rise.

Mangroves are typically distributed in the intertidal zone between Mean Sea Level (MSL) and high tide elevations (Lewis, 2005), it is very rare to find them at elevations much lower than MSL. Obviously, if mangrove shoreline can remain lasting seaward movement, this mean that elevation of the migration location in mangrove shoreline should be higher than that of MSL with little impacts from SLR. Thereof, our results about the robustly seaward migration of mangrove forest in the 4 deltas indicates that they can trap sediments to maintain their flat soil elevation to avoid mangrove dieback by SLR (Figure 3).

In the Indo-Pacific region over 28 deltas are present dominated by riverine, wave and tidal dynamics (Figure S13 in Supporting Information S1). Four typical deltas in the Northwest Pacific were selected to represent a wide range of tidal and wave conditions. Our study suggests that Northwest Pacific deltaic mangrove forests have been less affected by sea-level rise than previously expectation.

4.3. Relationship Between Mangrove Forest and Bare Tidal Flats

We also found that the seaward mangrove boundary where expansion occurs is often adjacent to broad bare tidal flats. The width of these flats can be as high as 2,800 m while the narrowest parts are still 100 m wide (Figures S6 and S8 in Supporting Information S1). Fast seaward mangroves expansion is associated to broad bare tidal flats, where the vegetation can easily encroach (Figure S14 in Supporting Information S1). Regions without bare tidal flats often display mangroves retreat, for example, the south part of the Mekong delta and the northeast part of the Beilun delta (Figures S7 and S8 in Supporting Information S1). Moreover, if the elevation in bare tidal flats does not match SLR, bare tidal flat deterioration will occur. When the bare flats retreat to the mangroves margin, the seaward expansion of the mangroves will stop. Therefore, there is close link between mangroves extension and

bare flats lateral progradation (Figure S15 in Supporting Information S1). Taken altogether, these observations mean that bare tidal flats control the process of mangroves development (Figures S14 and S15 in Supporting Information S1).

4.4. Future Changes in Deltaic Mangroves

The speed of global mangrove retreat in the face of SLR is of great concern around the world. There are two patterns of mangroves retreat: (a) the bare tidal flats in front of the mangroves are eroded away. Once mangroves lose the protection of the adjacent bare flats, they have to directly face currents and wave forcing, which can expose and undercut the forest roots, destabilize the trees, create erosion scarps that eventually result in mangroves retreat (Figure S8 in Supporting Information S1). (b) Bare tidal flats still expand seaward but vertical accretion cannot balance SLR, lowering the elevation below MSL. Thereafter the shorelines of mangrove and bare flat coincide with each other. Thus mangroves start to retreat, similar to the first pattern (Figure S16 in Supporting Information S1).

In the first configuration, erosion will occur at the ocean margin of the mangroves (Lovelock et al., 2015; Spencer et al., 2016). In the southern part of the Mekong delta, some seaward sites do not have a facing bare tidal flat and display mangrove loss (Figure 3, Figures S6 and S7 in Supporting Information S1), possibly caused by strong wave erosion that exposes mangrove roots and results in forest dieback. Similar seaward mangrove erosion can be found in the Red delta where wave heights range between 0.5 and 2.5 m (Figure 3, Table S10 in Supporting Information S1).

Meanwhile, a landward shift of tidal flooding location driven by SLR provides new space for mangroves expansion (Figure S16a in Supporting Information S1). If the bare tidal flat slope is lower than the upland slope, the area of potentially submerged mangroves due to SLR is larger than the area subject to landward expansion. In addition, the upland area is often occupied by shrimp ponds and agricultural levees, which limit the expansion area to a certain extent. Therefore landward expansion cannot compensate seaward loss of mangroves due to inundation. In this configuration, the ocean boundary of the mangroves is coincident with the bare tidal flat shoreline, and both retreat at the same time during SLR. However, the 4 deltas studied herein are still expanding seaward and therefore do not fall in this shoreline trajectory.

In the second configuration, bare tidal flats develop in front of the mangroves and they still expand seaward as sea level rises (Figure S16b in Supporting Information S1). The expansion rate of mangroves is closely related to the original bare tidal flat width and the change rate of bare tidal flat (Figures S13 and S14 in Supporting Information S1). Therefore, we include both bare tidal flats and mangrove dynamics in the conceptual model (Figures S16b and S16c in Supporting Information S1), and we determine the start of mangrove retreat under the low, intermediate and very high SLR scenarios published by IPCC (Figure S4 in Supporting Information S1). Model results suggest that mangroves in the 4 deltas can be able to survival for 410–720 years under future SLR (IPCC 6th Assessment Report) (Figure 4 and Table S8 in Supporting Information S1). The Nanliu delta may be submerged within 350–550 years, the Beilun delta in 420–470 years, the Red delta in 120–200 years, and the Mekong delta in 410–720 years, under the three selected IPCC scenarios (Figure S5 in Supporting Information S1). Approximately 75% of the mangrove forest will stop expanding within 80–110 years, while 90% may be submerged within 132–194 years (Figure 4). We project complete loss of the mangrove forest in 410–720 years (Figure 4) when the mangroves border reaches the bare tidal flat limit at approximately MSL.

We also found that when there are enough bare tidal flats in front of the mangroves and relatively small waves (such as in the Nanliu delta), the submergence time is shorter than deltas with strong wave energy (like the Beilun and Red deltas), this might be because low wave energy can favor growth of mangrove propagules (Figure 3, Figures S8, S17, and S18, Table S4 in Supporting Information S1). Therefore, wave energy and width of adjacent bare tidal flats may control the mangrove's seaward expansion.

5. Conclusions and Perspective

Mangrove forests serve as an important carbon sequestration ecosystem, and play a crucial role in storm protection (FAO, 2020; Friess et al., 2019). One km of mangroves can attenuate over 80% of storm surge (Zhou et al., 2022). Global warming will increase the risk of flooding by storm surges, and current dike systems designed for flood control may lose their efficacy. Mangrove forest can thus become the best natural defense system against

storms (Murray et al., 2022). Unfortunately, landward migration of mangrove forests is not possible due to the construction of anthropogenic barriers, like those present along the Indo-Pacific coast, and this ecosystem service might disappear. Removal of barriers to allow mangrove transgression is unlikely because these infrastructures are vital for the protection of agricultural fields and dwellings. Our study indicates that most deltaic mangroves are still migrating seaward. We insist that taking necessary measures to maintain the seaward expansion of mangroves can be an effective strategy for flood control, rather than demolition of existing sea dikes on the landward side. Specifically, we should promote the formation of bare tidal flats with suitable soil surface elevations, and create enough seaward migration space for mangroves encroachment. Prograding mangroves can also provide blue carbon sequestration and mitigate the impact of tropical storms. We believe that a nature-based shoreline defense can be realized by creating seaward space for mangrove expansion through appropriate siltation techniques and measures to promote the elevation of bare tidal flat.

Data Availability Statement

The hydrological data collected at BeiHai, HonDua, and VungTau gauging stations (Table S4 in Supporting Information S1) were provided by the Nation Oceanography Centre Permanent Service for Mean Sea Level (PSMSL) (https://psmsl.org/data/obtaining/) and the Mekong River Commission (MRC) (Data is available from https://www.mrcmekong.org/, upon registration/login). The used Landsat remote imageries were downloaded from the U.S. Geological Survey (https://glovis.usgs.gov/app?fullscreen=0).

Acknowledgments
This research was supported by the National Natural Science Key Foundation of China (NSFC) (41930537), National Key R&D Program of China (2023YFE0121200), and Shanghai International Science and Technology Cooperation Fund Project (23230713800); S.F. was partly funded by the USA National Science Foundation awards 2224608 (PIE LTER) and 1832221 (VCR LTER).

References

Aburto-Oropeza, O., Ezcurra, E., Danemann, G., Valdez, V., Murray, J., & Sala, E. (2008). Mangroves in the Gulf of California increase fishery yields. *Proceedings of the National Academy of Sciences of the United States of America*, *105*(30), 10456–10459. https://doi.org/10.1073/pnas.0804601105

Adame, M. F., Brown, C. J., Bejarano, M., Herrera-Silveira, J. A., Ezcurra, P., Kauffman, J. B., & Birdsey, R. (2018). The undervalued contribution of mangrove protection in Mexico to carbon emission targets. *Conservation Letters*, *11*(4), e12445. https://doi.org/10.1111/conl.12445

Adame, M. F., Neil, D., Wright, S. F., & Lovelock, C. E. (2010). Sedimentation within and among mangrove forests along a gradient of geomorphological settings. *Estuarine, Coastal and Shelf Science*, *86*(1), 21–30. https://doi.org/10.1016/j.ecss.2009.10.013

Amante, C. J., Love, M., Carignan, K., Sutherland, M. G., MacFerrin, M., & Lim, E. (2023). Continuously updated digital elevation models (CUDEMs) to support coastal inundation modeling. *Remote Sensing*, *15*(6), 1702. https://doi.org/10.3390/rs15061702

Asbridge, E., Lucas, R., Ticehurst, C., & Bunting, P. (2016). Mangrove response to environmental change in Australia's Gulf of Carpentaria. *Ecology and Evolution*, *6*(11), 3523–3539. https://doi.org/10.1002/ece3.2140

Blankespoor, B., Dasgupta, S., & Laplante, B. (2014). Sea-level rise and coastal wetlands. *Ambio*, *43*(8), 996–1005. https://doi.org/10.1007/s13280-014-0500-4

Dalrymple, R. W., Zaitlin, B. A., & Boyd, R. A. (1992). A conceptual model of estuarine sedimentation. *Journal of Sedimentary Petrology*, *62*(6), 1130–1146. https://doi.org/10.1306/d4267a69-2b26-11d7-8648000102c1865d

Duarte, C. M., Losada, I. J., Hendriks, I. E., Mazarrasa, I., & Marbà, N. (2013). The role of coastal plant communities for climate change mitigation and adaptation. *Nature Climate Change*, *3*(11), 961–968. https://doi.org/10.1038/nclimate1970

Duke, N. C., Meynecke, J. O., Dittmann, S., Ellison, A. M., Anger, K., Berger, U., et al. (2007). A world without mangroves? *Science*, *317*(5834), 41–42. https://doi.org/10.1126/science.317.5834.41b

Food and Agriculture Organization of the United Nations (FAO). (2007). The world's mangroves 1980–2005. In *FAO forestry paper*. FAO.

Food and Agriculture Organization of the United Nations (FAO). (2020). *Global forest resources assessment, 2020: Main report*. FAO.

Friess, D. A., Adame, M. F., Adams, J. B., & Lovelock, C. E. (2022). Mangrove forests under climate change in a 2°C world. *Climate Change*, de792. https://doi.org/10.1002/wcc.792

Friess, D. A., Rogers, K., Lovelock, C. E., Krauss, K. W., Hamilton, S. E., Lee, S. Y., et al. (2019). The state of the world's mangrove forests: Past, present, and future. *Annual Review of Environment and Resources*, *44*(1), 89–115. https://doi.org/10.1146/annurev-environ-101718-033302

Gandhi, S., & Jones, T. (2019). Identifying mangrove deforestation hotspots in South Asia, Southeast Asia and Asia-Pacific. *Remote Sensing*, *11*(6), 728. https://doi.org/10.3390/rs11060728

Giri, C., Ochieng, E., Tieszen, L. L., Zhu, Z., Singh, A., Loveland, T., et al. (2011). Status and distribution of mangrove forests of the world using earth observation satellite data. *Global Ecology and Biogeography*, *20*(1), 154–159. https://doi.org/10.1111/j.1466-8238.2010.00584.x

Godoy, M. D., & Lacerda, L. D. D. (2015). Mangroves response to climate change: A review of recent findings on mangrove extension and distribution. *Anais da Academia Brasileira de Ciências*, *87*(2), 651–667. https://doi.org/10.1590/0001-3765201520150055

Hamilton, S. E., & Casey, D. (2016). Creation of a high spatio-temporal resolution global database of continuous mangrove forest cover for the 21st century (CGMFC-21). *Global Ecology and Biogeography*, *25*(6), 729–738. https://doi.org/10.1111/geb.12449

Himmelstoss, E. A., Farris, A. S., Henderson, R. E., Kratzmann, M. G., Ergul, A., Zhang, O., et al. (2021). *Digital shoreline analysis system version 5.1*. U.S. Geological Survey software release.

Hu, Z., Zhou, J., Wang, C., Wang, H., He, Z., Peng, Y., et al. (2020). A novel instrument for bed dynamics observation supports machine learning applications in mangrove biogeomorphic processes. *Water Resources Research*, *56*(7), e2020WR027257. https://doi.org/10.1029/2020wr027257

IPCC. (2022). Climate change 2022: Impacts, adaptation, and vulnerability. In H.-O. Pörtner, D. C. Roberts, M. Tignor, E. S. Poloczanska, K. Mintenbeck, A. Alegría, et al. (Eds.), *Contribution of working group II to the sixth assessment report of the intergovernmental panel on climate change*. Cambridge University Press. https://doi.org/10.1017/9781009325844

Lewis, R. R. (2005). Ecological engineering for successful management and restoration of mangrove forests. *Ecological Engineering*, *24*(4), 403–418. https://doi.org/10.1016/j.ecoleng.2004.10.003

Long, C. Q., Dai, Z. J., Wang, R. M., Lou, Y. Y., Zhou, X. Y., Li, S. S., & Nie, Y. (2022). Dynamic changes in mangroves of the largest delta in northern Beibu Gulf, China: Reasons and causes. *Forest Ecology and Management*, *504*, 119855. https://doi.org/10.1016/j.foreco.2021.119855

Long, C. Q., Dai, Z. J., Zhou, X., Mei, X., & Van, C. M. (2021). Mapping mangrove forests in the red river delta, Vietnam. *Forest Ecology and Management*, *483*, 118910. https://doi.org/10.1016/j.foreco.2020.118910

Lovelock, C. E., Cahoon, D. R., Friess, D. A., Guntenspergen, G. R., Krauss, K. W., Reef, R., et al. (2015). The vulnerability of Indo-Pacific mangrove forests to sea-level rise. *Nature*, *526*(7574), 559–563. https://doi.org/10.1038/nature15538

Lovelock, C. E., Sorrell, B. K., Hancock, N., Hua, Q., & Swales, A. (2010). Mangrove forest and soil development on a rapidly accreting shore in New Zealand. *Ecosystems*, *13*(3), 437–451. https://doi.org/10.1007/s10021-010-9329-2

McIvor, A. L., Spencer, T., Möller, I., & Spalding, M. (2013). The response of mangrove soil surface elevation to sea level rise. Natural Coastal Protection Series: Report 3. Cambridge Coastal Research Unit Working Paper 42. ISSN 2050-7941.

McKee, K. L., Cahoon, D. R., & Feller, I. C. (2007). Caribbean mangroves adjust to rising sea level through biotic controls on change in soil elevation. *Global Ecology and Biogeography*, *16*(5), 545–556. https://doi.org/10.1111/j.1466-8238.2007.00317.x

Milliman, J. D., & Farnsworth, K. L. (2011). *River discharge to the coastal ocean – A global synthesis*. Cambridge University Press.

Morris, J. T., Sundareshwar, P. V., Nietch, C. T., Kjerfve, B., & Cahoon, D. R. (2002). Responses of coastal wetlands to rising sea level. *Ecology*, *83*(10), 2869–2877. https://doi.org/10.2307/3072022

Murray, N. J., Phinn, S. R., DeWitt, M., Ferrari, R., Johnston, R., Lyons, M. B., et al. (2019). The global distribution and trajectory of tidal flats. *Nature*, *565*(7738), 222–225. https://doi.org/10.1038/s41586-018-0805-8

Murray, N. J., Worthington, T. A., Bunting, P., Duce, S., Hagger, V., Lovelock, C. E., et al. (2022). High-resolution mapping of losses and gains of Earth's tidal wetlands. *Science*, *376*(6594), 744–749. https://doi.org/10.1126/science.abm9583

Saintilan, N., Horton, B., Törnqvist, T. E., Ashe, E. L., Khan, N. S., Schuerch, M., et al. (2023). Widespread retreat of coastal habitat is likely at warming levels above 1.5°C. *Nature*, *621*(7977), 112–119. https://doi.org/10.1038/s41586-023-06448-z

Schuerch, M., Spencer, T., Temmerman, S., Kirwan, M. L., Wolff, C., Lincke, D., et al. (2018). Future response of global coastal wetlands to sea-level rise. *Nature*, *561*(7722), 231–234. https://doi.org/10.1038/s41586-018-0476-5

Spencer, T., Schuerch, M., Nicholls, R. J., Hinkel, J., Lincke, D., Vafeidis, A. T., et al. (2016). Global coastal wetland change under sea-level rise and related stresses: The DIVA wetland change model. *Global and Planetary Change*, *139*, 15–30. https://doi.org/10.1016/j.gloplacha.2015.12.018

Syvitski, J. P. M., Kettner, A. J., Overeem, I., Hutton, E. W. H., Hannon, M. T., Brakenridge, G. R., et al. (2009). Sinking deltas due to human activities. *Nature Geoscience*, *2*(10), 681–686. https://doi.org/10.1038/ngeo629

Tamura, T., Nguyen, V. L., Ta, T. K. O., Bateman, M. D., Gugliotta, M., Anthony, E. J., et al. (2020). Long-term sediment decline causes ongoing shrinkage of the Mekong megadelta, Vietnam. *Scientific Reports*, *10*(1), 8085. https://doi.org/10.1038/s41598-020-64630-z

Willemsen, P. W. J. M., Horstman, E. M., Borsje, B. W., Friess, D. A., & Dohmen-Janssen, C. M. (2016). Sensitivity of the sediment trapping capacity of an estuarine mangrove forest. *Geomorphology*, *273*, 189–201. https://doi.org/10.1016/j.geomorph.2016.07.038

Woodroffe, C. D., Rogers, K., McKee, K. L., Lovelock, C. E., Mendelssohn, I. A., & Saintilan, N. (2016). Mangrove sedimentation and response to relative sea-level rise. *Annual Review of Marine Science*, *8*(1), 243–266. https://doi.org/10.1146/annurev-marine-122414-034025

Worthington, T. A., Zu Ermgassen, P. S., Friess, D. A., Krauss, K. W., Lovelock, C. E., Thorley, J., et al. (2020). A global biophysical typology of mangroves and its relevance for ecosystem structure and deforestation. *Scientific Reports*, *10*(1), 14652. https://doi.org/10.1038/s41598-020-71194-5

Zhou, X. Y., Dai, Z. J., Carniello, L., Long, C. Q., Wang, R., Luo, J. J., & Huang, Z. M. (2022). Linkage between mangrove wetland dynamics and wave attenuation during a storm–a case study of the Nanliu Delta, China. *Marine Geology*, *454*(2022), 106946. https://doi.org/10.1016/j.margeo.2022.106946

References From the Supporting Information

Baloloy, A. B., Blanco, A. C., Raymund Rhommel, R. R. C., & Nadaoka, K. (2020). Development and application of a new mangrove vegetation index (MVI) for rapid and accurate mangrove mapping. *ISPRS Journal of Photogrammetry and Remote Sensing*, *166*, 95–117. https://doi.org/10.1016/j.isprsjprs.2020.06.001

Gao, B. C. (1996). NDWI—A normalized difference water index for remote sensing of vegetation liquid water from space. *Remote Sensing of Environment*, *53*(3), 257–266. https://doi.org/10.1016/s0034-4257(96)00067-3

Huete, A., Didan, K., Miura, T., Rodriguez, E. P., Gao, X., & Ferreira, L. G. (2002). Overview of the radiometric and biophysical performance of the MODIS vegetation indices. *Remote Sensing of Environment*, *83*(1–2), 195–213. https://doi.org/10.1016/s0034-4257(02)00096-2

Rouse, J. W., Haas, R. H., Scheel, J. A., & Deering, D. W. (1974). Monitoring vegetation systems in the great plains with ERTS. In *Proceedings, 3rd earth resource Technology satellite (ERTS) symposium* (Vol. 1, pp. 48–62).